

# Preparation and Characterization of Glyceryl monostearate Solid

## Lipid Nanoparticles by High Shear Homogenization.

### Authors:

Ahmed R. Gardouh<sup>1</sup>, Shadeed G. abdelrahman<sup>1</sup>, Hassan M. Ghonaim<sup>1,2</sup> and MamdouhM<sup>1</sup>.  
Ghorab

1 Department of Pharmaceutics and Industrial Pharmacy, Faculty of Pharmacy, Suez Canal University, Ismailia 41522, Egypt.

2 Institute of Life Sciences Research, University of Bradford, Bradford, BD7 1RD, UK.

Corresponding author: hassan\_ghonaim@pharm.suez.edu.eg

### ABSTRACT

**Aims:** The aim of this study was to explore the practicability of preparation of solid lipid nanoparticles of glycerylmonostearatecontaining dibenzoyl peroxide, erythromycin base, and triamcinolone acetonide as model drugs. The physicochemical properties of the prepared formulae like particle size, drug entrapment efficiency, drug loading capacity, yield content and in-vitro drug release behavior were characterized.

**Methods:** Solid lipid nanoparticles loaded with three model lipophilic drugs were prepared by high shear hot homogenization method. The model drugs used are dibenzoyl peroxide, erythromycin base, and triamcinolone acetonide. glycerylmonostearate was used as lipid core. tween 20 and tween 80 were employed as surfactants and lecithin as co-surfactant. Many formulation parameters were controlled to obtain high quality nanoparticles. The prepared solid lipid nanoparticles were evaluated by different standard physical and imaging methods. The efficiency of drug release form prepared formulae was studied using *in vitro* technique with utilize of dialysis bag technique. The stability of prepared formulae was studied by thermal procedures and infrared spectroscopy.

**Results:** The mean particle diameter measured by laser diffraction technique was  $194.6 \pm 5.03$  to  $406.6 \pm 15.2$  nm for dibenzoyl peroxide loaded solid lipid nanoparticles,  $220 \pm 6.2$  to  $328.34 \pm 2.5$  for erythromycin loaded solid lipid nanoparticles and  $227.3 \pm 2.5$  to  $480.6 \pm 24$  for triamcinolone acetonide loaded solid lipid nanoparticles. The entrapment efficiency and drug loading capacity, determined with UV spectroscopy, were  $80.5 \pm 9.45\%$  and  $0.805 \pm 0.093\%$ , for dibenzoyl peroxide,  $96 \pm 11.5$  and  $0.96 \pm 0.012$  for triamcinolone acetonide and  $94.6 \pm 14.9$  and  $0.946 \pm 0.012$  for erythromycin base respectively. It was found that model drugs showed significant faster release patterns when compared with commercially available formulations and pure drugs ( $p < 0.05$ ). Thermal analysis of prepared solid lipid nanoparticles gave indication of solubilization of drugs within a lipid matrix. FTIR Spectroscopy showed the absence of new bands for loaded solid lipid nanoparticles indicating no interaction between drugs and lipid matrix and being only dissolved

in it. Electron microscope of scanning and transmission techniques indicated sphere form of prepared solid lipid nanoparticles with smooth surface with size below 100 nm.

**Conclusions:** Solid lipid nanoparticles with small particle size, high encapsulation efficiency, and relatively high loading capacity for dibenzoyl peroxide, erythromycin base, and triamcinolone acetonide can be obtained by this method.

**Key Words:** Solid lipid nanoparticles, High shear homogenization, Tween 20, Tween 80, Glycerylmonostearate, Dibenzoyl peroxide, Erythromycin base, Triamcinolone acetonide.

## 1. INTRODUCTION

Solid lipid nanoparticles (SLN) offer an attractive means of drug delivery, particularly for poorly water-soluble drugs. They combine the advantages of polymeric nanoparticles, fat emulsions and liposomes (Schwarz et al., 1994). SLN consist of drug trapped in biocompatible lipid core and surfactant at the outer shell, offering a good alternative to polymeric systems in terms of lower toxicity (Muller et al., 2000). Moreover, the production process can be modulated for desired drug release, protection of drug degradation and avoidance of organic solvents. The previous advantages make SLN a promising carrier system for optimum drug delivery. dibenzoyl peroxide is a safe and effective agent for treating acne. (Gupta et al., 2003). Furthermore, dibenzoyl peroxide's lipophilic nature enhances transport through sebaceous glands, with maximum penetration through acne follicles. Dibenzoyl peroxide can be attached to the solid lipid nanoparticles surface and facilitate drug targeting to skin strata and increase efficiency of acne remedy (Stecova et al., 2007).

Topical erythromycin treatment was used for inflammatory acne vulgaris due to activity against *Propionibacterium acnes* (Schafer- Korting et al., 2007). It is slightly soluble in water, freely soluble in alcohol, soluble in methanol.

Triamcinolone acetonide is a topical lipophilic corticosteroid used to treat dermatitis (Yang et al., 2006). Dibenzoyl peroxide, erythromycin base and triamcinolone acetonide are examples of topical drugs with poor dermal localization due to lipophilicity. Solid lipid nanoparticles could be a carrier for these drugs with potential impact on the dissolution of these drugs.

The aim of this study was to explore the practicability of preparation of solid lipid nanoparticles containing dibenzoyl peroxide (DP), erythromycin base (ER), and triamcinolone acetonide (TA). High shear hot homogenization technique was employed to prepare the solid lipid nanoparticles; the physicochemical properties of the SLNs like particle size, drug entrapment efficiency (EE), drug loading capacity (LC), yield content and in-vitro drug release behavior were studied.

## 2. METHODOLOGY

## 2.1. Materials

Glyceryl monostearate-technical self-emulsifying (BDH Chemicals Ltd Poole- England), Tween 80 (polysorbate 80), Tween 20 (polysorbate 20) , ICI America (Wilmington, DE, USA) , Lecithin (Spectrum Chemicals & Laboratory Products, New Brunswick, NJ), Dibenzoyl peroxide, triamcinolone acetonide, erythromycin base (gift from MUP pharmaceutical company, Abu sultan, Egypt), Akenemycin<sup>®</sup> cream , Akenroxide<sup>®</sup> gel (MUP pharmaceutical company, Abusultan, Egypt) ,Kenalog<sup>®</sup> cream (Bristol–Myerssquib) , Dialysis tubing cellulose membrane (molecular weight cut-off 12,000 g/mole) sigma-Aldrich Chemical Company, St.Louis, USA, and all other chemicals were of reagent grade and used as delivered.

## 2.2. Methods

### 2.2.1. Preparation of solid lipid nanoparticles loaded with model drugs:

Solid lipid nanoparticles of the smallest size during the preliminary study were loaded with DP, ER and TA as model topical drugs. Briefly, the drugs were dispersed in melted lipid (60- 70<sup>0</sup>), then the mixture was dispersed in a hot aqueous solution with surfactant concentration of 5 % w/w and 1 % w/w lecithin as co-surfactant at the same temperature, by high –speed stirring, using an Ultra-Turrax homogenizer (Ultra- Turrax T – 25, IKA, Germany) at 12, 000 rpm for 10 minutes, with 30 seconds intervals every two minutes. The resulting dispersion was then cooled and each sample was diluted with water before the measurement and particle size was measured using dynamic laser light scattering apparatus at 25<sup>0</sup>C. (Mastersizer 2000 vers. 5.54, hydro 2000 S, Malvern instruments Ltd., Malvern, Worcs, UK). Each measurement was performed in triplicate and the average particle diameter and polydispersity index (PI) were determined (Mehnert et al., 2001). SLNs were prepared by the same technique using 50 % w/w glycerol as viscosity enhancer.

### 2.2.2. Loading capacity:

The loading capacity (L.C) refers to the percentage amount of drug entrapped in solid lipid nanoparticles according to the following equation:

$$\text{L.C.} = \frac{\text{Total amount of drug} - \text{amount of unbound drug}}{\text{Nanoparticles weight}} \times 100$$

### 2.2.3. Encapsulation efficiency:

Drug entrapment efficiency was determined by ultracentrifugation. The drug entrapment efficiency was calculated from the ratio of the drug amount incorporated into SLNs to the total added drug amount. Ultracentrifugation was carried out using ultracentrifuge (Eppendorf centrifuge 5417 C, Netheler- Hinz- Gmbh), About 1 gm of SLNs dispersion containing the drug was placed in the centrifuge tube, and samples were centrifuged at 14,000 rpm for 15 min. The amount of the drug in the supernatant was estimated spectrophotometrically at 235 NM for DP according to (B.P 2009), 250nm for TA according to (B.P 2009) and 633 NM against a blank after ion pair with crystal violet for ER (Amin et al., 1996).

$$\text{Total amount of drug} - \text{amount of unbound drug}$$

$$\text{E.E.} = \frac{\text{Total amount of drug}}{\text{Total amount of drug}} \times 100$$

#### 2.2.4. **Determination of yield of solid lipid nanoparticles:**

This was calculated by weighing centrifuged samples of isolated solid lipid nanoparticles and referring them to the initial amount of solid lipid nanoparticles components according to the following equation

$$\text{Yield percentage (Y.P)} = \frac{\text{SLNs weight}}{\text{Total initial solids weight}} \times 100$$

Table (1): Composition of Selected Formulas Used For Loading of Model Drugs.

Formula code	GMS %w/w	Co-surfactant		Glycerol %w/w
		Surfactant % w/w	% w/w (lecithin)	
F1	10.0	5.0 (Tween 80)	1.0	-----
F2	10.0	5.0 (Tween 80)	1.0	50.0
F3	10.0	5.0 (Tween 20)	1.0	-----
F4	10.0	5.0 (Tween 20)	1.0	50.0

#### 2.2.5. **Scanning Electron Microscopy (SEM):**

For scanning electron microscopy (SEM), dried solid lipid nanoparticles loaded with model drugs were fixed on a brass stub using double-sided adhesive tape and then made electrically conductive by coating with a thin layer of gold for 30 seconds using JEOL fine coat (JFC-1100F ion sputtering device) and scanned using JEOL (JSM-S.M 5300) using software (ORION 6.60.4).

#### 2.2.6. **Transmission Electron Microscopy (TEM):**

Solid lipid nanoparticles loaded with model drugs were stained with phosphotungstic acid 2% w/v and placed on copper grids with Formvar films for viewing by a transmission electron



microscope operated at 120 kv (JEOL-JEM-100CX EM) and operated using computer program named (AMT Image Capture Engine V601)

#### **2.2.7. Differential Scanning Calorimetry (DSC):**

Accurately weighed samples (1-8) mg samples were crimped in closed 40- $\mu$ l aluminum pans. Samples were run at a heating rate of 10 °C /min under constant purging of nitrogen at 30 ml/ min and heated from 25.0 °C to 300.0 °C (except for samples of GMS, it was heated to only 80 °C and samples of DP to only 200 °C) using Shimadzu DSC-60, Kyoto, Japan and Shimadzu DSC-60 data analysis. The references used for comparison were the same but empty aluminum pans.

#### **2.2.8. Fourier Transformation Infrared Spectroscopy (FTIR):**

The pure drug, plain dried solid lipid nanoparticles, physical mixture and model drug loaded dried solid lipid nanoparticles were mixed for each with KBr (IR grade) in the ratio of 100: 1 and then scanned over a wave number range 4000- 500  $\text{cm}^{-1}$ .

#### **2.2.9. In- vitro drug release studies:**

These studies were completed using a horizontal water bath shaker (Clifton water bath, USA) that maintained at 60 cycles per minute and the dialysis bag that could retain SLNs and allow the diffusion of free drug into dissolution media. The bags were soaked in distilled water for 12 h before use. The release medium was 10 ml phosphate buffer (pH 5.5). The temperature was set at  $32 \pm 0.5$  °C. A 1gm sample of the drug loaded SLNs was installed in a dialysis bag held with two clamps at each end. At known time intervals (0.5, 1, 2, 4, 8, 12, 24, 36, and 48 h) the complete media were withdrawn and replaced by equal volumes of fresh buffer to maintain sink condition. The samples filtered and assayed for each model drug spectrophotometrically. The experiments were carried out as triplicate for each release study and the mean values were calculated (Feng et al., 2008).

#### **Statistical analysis:**

- All data were expressed as mean  $\pm$  SD.
- Data were analyzed by using the program SPSS 16.0 (SPSS Inc., Chicago, IL, USA) with the help of one-way analysis of variance (ANOVA) test followed by post hoc multiple comparisons and (LSD) least significant difference formulae, significant at  $P < 0.05$ .

### **3. RESULTS AND DISCUSSION**

### **3.1. Particle Size of Prepared Solid Lipid Nanoparticles:**

Solid lipid nanoparticles of selected formulations listed in table (1) were loaded with model drugs were prepared using high shear hot homogenization with 12,000 rpm as homogenization speed.

Table (2) showed that the mean particle size measured by a laser diffraction technique was  $194.6 \pm 5.03$  to  $406.6 \pm 15.2$  NM for Dibenzoyl peroxide loaded solid lipid nanoparticles,  $220 \pm 6.2$  to  $328.34 \pm 2.5$  for Erythromycin loaded solid lipid nanoparticles and  $227.3 \pm 2.5$  to  $480.6 \pm 24$  for Triamcinolone acetonide loaded solid lipid nanoparticles; while for empty solid lipid nanoparticles, particle size was from  $172 \pm 3$  NM to  $231 \pm 11$  NM. It was found that loading did not affect the size of solid lipid nanoparticles. This result was in agreement with (Vivek et al., 2007) who found that lipid hydrophilicity, self-emulsifying properties of the lipid affected the shape of the lipid crystals (and hence the surface area) that had an indirect effect on the final size of the SLN dispersions. These results agreed with (Le Verger et al., 1998) who compared empty nanoparticles with that loaded with isradipine and found no significant difference between empty and loaded nanoparticles; solubility or dispersion of model drugs into nanoparticles beside high concentration of surfactant and co-surfactant may be a good reason for that. These results agreed with that of (Almeida et al., 1997) who stated that solid lipid nanoparticles are appropriate to incorporate lipophilic drugs that are dissolved in melted lipid.

Table (2): Particle Size and Polydispersity Index of Empty SLNs and Loaded SLNs.

Formula code	Empty SLNs		DP-SLNs		ER-SLNs		TA-SLNs	
	Particle size $\pm$ S.D	P.I	Particle size $\pm$ S.D	P.I	Particle size $\pm$ S.D	P.I	Particle size $\pm$ S.D	P.I
F1	187 $\pm$ 0.57	0.003	286 $\pm$ 15.7	0.054	234 $\pm$ 9.6	0.041	429 $\pm$ 18	0.0419
F2	172 $\pm$ 3	0.0104	194.6 $\pm$ 5.03	0.0371	220 $\pm$ 6.2	0.028	227.3 $\pm$ 2.5	0.0109
F3	231 $\pm$ 11	0.026	406.6 $\pm$ 15.2	0.0376	273 $\pm$ 10.5	0.008	480.6 $\pm$ 24	0.0499
F4	180 $\pm$ 1	0.007	356 $\pm$ 13.5	0.0378	328.34 $\pm$ 2.5	0.0109	352.67 $\pm$ 7.6	0.030

### **3.2. Encapsulation Efficiency, Loading Capacity, and Yield Content:**

Table (3) showed high relative encapsulation efficiency and drug loading relative to theoretical values. This may be due to high lipid concentration that enhances solubility of drugs and so loading of them into SLNs. These results agreed with that of (Bhalekar et al., 2009). The encapsulation efficiency in most formulations > 75% which may be due to higher ratio of lipid to drug (5:1). These results agreed with (Kim et al., 2005) who found that loading of verapamil drug was > 75 % for all formulations having high lipid to verapamil ratio (5:1 and 10:1). The results showed high encapsulation efficiency and drug loading for formulations F1 and F3 relative to F2 and F4; that may be attributed to the high viscosity of formulations F2 and F4. The presence of 50 % glycerol in previous formulae may hinder the loading of drugs into SLNs due to the retardation of movement of particles. The encapsulation efficiency and drug loading of formulae F1 and F2 higher than F3 and F4, respectively due to use of Tween 80 with higher HLB than Tween 20 used for other formulae. Higher HLB values may enhance loading and encapsulation efficiency depending on reduction of interfacial tension and enhancement of solubilization of model drugs. These results were not in agreement with that of (El-laithy et al., 2011) who prepared Vinpocetine emulsions and found that the resulted product showed high encapsulation efficiency regardless of HLB of nonionic surfactants.

Table (3): Yield percentage (Y.P), Encapsulation efficiency (E.E) and Loading capacity (L.C) of Loaded SLNs.

Formula code	DP-SLNs			ER-SLNs			TA-SLNs		
	Y.P %	E.E %	L.C (ratio)	Y.P %	E.E %	L.C (ratio)	Y.P %	E.E %	L.C (ratio)
F1	69.72±1.69	77.26±4.06	0.7726±0.031	79.68±22.9	94.6±14.9	0.946±0.012	49.8±5.09	96±11.5	0.96±0.012
F2	49.8±5.36	51.23±6.85	0.5123±0.061	39.8±13.8	83.06±7.95	0.8306±0.09	19.9±6.12	89.3±12.9	0.893±0.058
F3	49.8±8.92	80.5±9.45	0.805±0.093	59.7±6.12	85.04±5.24	0.8504±0.054	39.8±7.49	85.34±7.44	0.8534±0.025
F4	39.8±2.91	51.23±8.61	0.5123±0.0211	29.88±5.14	74.9±6.92	0.749±0.091	10.9±3.94	75.3±6.08	0.753±0.031

### **3.3. In-vitro Release Study:**

Membrane diffusion techniques are widely used for the study of drug in vitro release incorporated in colloidal systems. In these cases, drug release follows more than one mechanism. In case of release from the surface of SLNs, adsorbed drug quickly dissolved when it comes in contact with the release medium. Drug release by diffusion involves three steps. Briefly, water penetrates into system and causes swelling of matrix followed by the conversion of solid lipid into a rubbery matrix, and then the diffusion of drugs from the swollen rubbery matrix takes place. Hence, the release is slow initially and later, it becomes fast (Agnihotri et al., 2004).

According to (Le Verger et al., 1998) the release rate of the drug and its appearance in the dissolution medium is controlled by partitioning the drug between the lipid phase and the aqueous environment in the dialysis bag then by diffusion of the drug across the membrane.

The mode of preparation (cold or hot homogenization) influences the drug release profile. It was noted by (Schafer –Korting et al., 2007) that surfactant and higher temperature enhanced prednisolone solubility in the aqueous phase and supported the enrichment of the steroid in the superficial layers during cooling of the preparation and crystallization of the lipid. Superficially entrapped prednisolone is available for the initial burst release.

Figures (1-3) showed that the release of drugs from formulae was enhanced significantly at level of  $P < 0.05$  when compared with drugs only, drugs mixed Tween 80 and drugs mixed with Tween 20 with the same proportions as in the formulae and also commercially available formulations.

Upon comparing the release of model drugs from prepared formulae, it was found that formula F1 better release efficiency than F3. Tween 80 used for the preparation of F1 gave smaller size than that of Tween 20 used for the preparation of formula F3 with larger micelle size but with lower solubilizing capacity of lipophilic drugs, and hence lower dissolution rate that result in lower release efficiency (Ghorab et al., 2004).

The effect of viscosity (50 % Glycerol) on the release of model drugs from prepared formulae were studied as seen in figures (1-3). Glycerol was used as a viscosity enhancer during earlier optimization of conditions for SLNs preparation, and resulted in smaller size for the formulae F2 and F4. During release studies, release efficiency of drugs from formulae F1 and F3 were better than that of F2 and F4 that contain 50 % glycerol. Formulae F2 and F4 had a consistency of semisolid form while F1 and F3 still in liquid form which had a good relation to effect of viscosity on release of drugs. According to (Bisrat et al., 1992) who found that the viscosity of glycerol affected the rate of dissolution and diffusion of griseofulvin that compatible with our results.

### **3.4. Scanning Electron Microscopy (SEM):**

After loading of different formulations with model drugs, in vitro release studies revealed that formulation F1 showed significant enhancement of release for all model drugs. The formulation

showed best in vitro release discussed earlier were scanned using scanning electron microscope to evaluate the surface of formulating solid lipid nanoparticles. Figures (4-6) showed illustrated scans of formulated SLNs loaded with models drugs. From these scans, all SLNs are spherical in shape with smooth surfaces.

### **3.5. Transmission Electron Microscope (TEM):**

Figures (7-9) show the shape of the nanoparticles entrapping DP, ER and TA. The particles tested demonstrated round and homogeneous shape; the figures also made us sure that the prepared SLNs size was less than 100 NM which agreed with the results of (Han et al., 2008) who prepared ministering nanostructured lipid carriers and studied TEM and found that the particles investigated were round with homogeneous shading and particle size ranging from 50 to 100 nm. The figures illustrated the presence of a layer enclosing the nanoparticles which is characteristic in the case of loaded SLNs. These results in full agreement with (Sznitowska et al., 2001) as they studied the TEM of diazepam loaded SLNs and found a layer around loaded SLNs that was not apparent in unloaded ones. This is also in agreement with other results of (Muller et al., 2000) (Muhlen et al., 1998) and (Muhlen et al., 1998).

It can be fulfilled that the values of SLNs diameters by TEM were clearly smaller than those measured by the particle size analyzer. This may be ascribed to dehydration of nanoparticles during sample preparation for TEM. Also, the particle size analyzer measures the apparent size (hydrodynamic radius) of particles including hydrodynamic layers that form around these nanoparticles leading to overestimation of the nanoparticles size (Motwani et al., 2008) and (Prabha et al., 2002).

### **3.6. Fourier Transformation Infrared Spectroscopy:**

Fig (10) showed the FTIR spectrum of GMS (lipid core and main component of SLNs). The characteristic bands of it showed C-H stretching and C-H bending at  $1200-1000\text{ cm}^{-1}$  and  $850-700\text{ cm}^{-1}$  (Pretsch et al., 2000).

Fig (11) showed the FT-IR of DP, physical mixture and DP-SLNs. The characteristic bands of DP include medium weak doublet band of O-O at  $1017-880\text{ cm}^{-1}$ , strong band of C-O-O at  $1200-1000\text{ cm}^{-1}$ , characteristic aromatic C-H at  $3400-3000\text{ cm}^{-1}$  and characteristic peak of benzoyl groups at  $1727\text{ cm}^{-1}$ . The absence of new bands of DP-SLNs indicated no interaction between drug and lipid matrix, and drug being only dissolved in matrix (Pretsch et al., 2009).

Figure (12) showed the FT-IR of ER and ER-SLNs which reveal differences in three regions ( $3300-3700$ ,  $2900-3000$ , and  $1600-1800\text{ cm}^{-1}$ ). The small shoulder in the region of  $2900-3000\text{ cm}^{-1}$  may be due to the effect of water presented in the molecules on alkane stretching. The difference in intensities of two peaks in the region between  $1600$  and  $1800\text{ cm}^{-1}$  suggests the difference in orientation of carbonyl groups. The absence of new bands of ER-SLNs indicated that there was no chemical reaction between the drug and lipid matrix, being only dissolved in a

lipid matrix of GMS. These results were in full agreement with that obtained from Sarisuta et al, (Sarisuta et al., 1999) who studied the FT-IR of ER loaded on different formulations.

In FT-IR spectrum (Fig. 13), the characteristic bands observed from the data of TA included the OH group in the range  $3650\text{--}3200\text{cm}^{-1}$ , C–H stretching in the range of  $3000\text{cm}^{-1}$  and  $2900\text{cm}^{-1}$ , C=O in  $1775\text{--}1650\text{cm}^{-1}$ , C=C in  $1690\text{--}1635\text{cm}^{-1}$ , and C–O–C in  $1310\text{--}1000\text{cm}^{-1}$  (Pretsch et al., 2000). The absence of new bands for TA-SLN gave indication that there was no chemical interaction between the drug and the lipid, being drug only dissolved in the lipid matrix. Similar results were documented by (Da Silva-Junior et al., 2009) for triamcinolone loaded formulations.

### **3.7. Differential Scanning Calorimetry (DSC) :**

The Formula F1 used for loading model drugs due to best release of model drugs was thermally scanned using differential scanning calorimetry (DSC). Figure (14) showed DSC thermogram of GMS (main constituent of solid lipid nanoparticles) with sharp endothermic peak around  $60^{\circ}\text{C}$ , indicative of melting. These results agreed with that of (Freitas et al., 1999) who studied the DSC analysis of GMS and found that melting endotherm of it was at  $60.39^{\circ}\text{C}$ . Figure (15) showed DSC Thermograms of plain SLNs (Formula F1) with a characteristic peak of GMS reduced to be at  $50^{\circ}\text{C}$  approximately. The shift of melting point of GMS may be due to small size (nanometer range) of SLNs compared with lipids in bulk, the dispersed condition of the lipid, and use of surfactants. These results augmented by other literatures (Muhlen et al., 1998), (Reddy et al., 2005) and (Bunjes et al., 1996).

Figure (16) showed DSC thermograms of DP, a physical mixture of drug and GMS and DP-SLNs. The thermogram of DP showed a very short endothermic peak at  $104^{\circ}\text{C}$  followed by sharp exothermic peak around  $117^{\circ}\text{C}$  which indicated that the drug was melted followed by degradation. Physical mixture formed of model drug and GMS only. The DSC thermogram of physical mixture showed the characteristic peaks of both GMS at  $56^{\circ}\text{C}$  with melting and degradation peaks of DP.

DSC thermogram of DP-SLNs was characterized by initial endothermic peak at  $50^{\circ}\text{C}$  approximately which is characteristic for GMS with absence of characteristic exothermic peak of DP which may be indicative of absence of drug in crystalline form and solubilization of drug within the lipid matrix with enhanced stability.

Fig (17) showed DSC thermograms of ER, physical mixture and ER-SLNs (formula F1). The DSC thermogram of ER showed characteristic endothermic peaks at  $188^{\circ}\text{C}$ ,  $257^{\circ}\text{C}$  and  $294^{\circ}\text{C}$  indicating degradation of drug. DSC thermogram of physical mixture containing ER showed a characteristic peak of GMS at  $57^{\circ}\text{C}$  with that of ER endothermic peak at  $188^{\circ}\text{C}$ ,  $257^{\circ}\text{C}$  and  $294^{\circ}\text{C}$ .

DSC thermogram of ER-SLNs showed the characteristic peak of GMS that shifted to about  $50^{\circ}\text{C}$  with absence of endothermic peak of ER indicating solubilization of drug in the lipid matrix of formulated solid lipid nanoparticles.

Fig (18) showed DSC thermograms of TA, physical mixture and TA-SLNs (formula F1).



The DSC thermogram of TA showed a characteristic sharp endothermic peak at 288 °C approximately indicating melting of the drug. The DSC analysis of the physical mixture (prepared in the same manner of previous drugs) showed both characteristic peaks of GMS at 60°C and of that of TA at 288 °C. DSC endotherm of TA-SLNs revealed only the characteristic peak of GMS with the absence of that of TA indicating solubilization within a lipid matrix. These results were incomplete fit with that results obtained from (Araujo et al., 2010).

#### **4. CONCLUSION**

In this study, lipophilic model drugs (Dibenzoyl peroxide, Erythromycin base and Triamcinolone acetonide) were used to study the feasibility of preparation of solid lipid nanoparticles. The drugs were successfully incorporated into SLNs by high-shear hot homogenization technique. The effects of different formulation parameters like viscosity and surfactant type and concentration on encapsulation efficiency, particle size and physicochemical properties of produced SLNs were investigated. Drug release from prepared SLNs formulae was enhanced compared to commercially available formulae as obtained through in vitro release tests. The type of surfactant and also concentration beside glycerol as a viscosity enhancer used had a great power of the physicochemical description of SLNs and the in vitro drug release. Formulation F1 containing Tween 80 as a surfactant and the lipid matrix (10% Glyceryl monostearate and 5% Tween 80 with 1 % lecithin as co-surfactant) showed the best results according to the entrapment efficiency and in vitro drug release.

#### **ACKNOWLEDGMENT**

The authors are grateful for Suez Canal University for funding the research and MUP Pharmaceutical Company for providing the active ingredient.

#### **COMPETING INTERESTS**

Authors have declared that no competing interests exist.

#### **REFERENCES**

- Agnihotri, S. A., Mallikarjuna, N. N., Aminabhavi, T. M. (2004). Recent advances on chitosan-based micro- and nanoparticles in drug delivery . J. Control. Rel. 1,5-28.
- Almeida, A.J., Runge, S., Muller, R.H. (1997). peptide –loaded solid lipid Nanoparticles (SLN): influence of production parameters. Int. J. Pharm. 149, 255- 265.
- Amin, A.S., Issa, Y.M. (1996). Selective spectrophotometric method for the determination of erythromycin and its esters in pharmaceutical formulations using gentian violet. J. Pharm. Biomed. Anal. 14, 1625- 1629.

- Araujo,J., Mira-Gonzalez, E., Egea,M.A., Garcia,M.L., Souto,E.B. (2010).Optimization and physicochemical characterization of a triamcinolone acetone-loaded NLC for ocular antiangiogenic applications. *Int.J.Pharm.* 393, 167-175.
- Bhalekar,M.R.,Pokharkar,V., Madgulkar,A.,Patil,N. (2009).Preparation and Evaluation of Miconazole Nitrate-Loaded Solid Lipid Nanoparticles for Topical Delivery. *AAPS PharmSciTech*, 10(1): 289-296.
- Bisrat,M., Anderberg,E. K.,Barnett,M. I., Nyström,C.(1992).Physicochemical aspects of drug release. XV. Investigation of diffusional transport in dissolution of suspended, sparingly soluble drugs .*Int. J. Pharm.* 80(1-3),191-201.
- British pharmacopoeia. (2009). Commission office.British pharmacopoeia. The stationary office, London.
- Bunjes,H.,Westesen,K.,Koch,M. H. J.(1996). Crystallization tendency and polymorphic transitions in triglyceride nanoparticles.*Int. J. Pharm.* 129, 159–173.
- Da Silva-Junior, A.A., De Matos, J.R., Formariz, T.P., Rossanezi,G., Scarpa, M.V., Do Egito,E.S.T., De Oliveira, A.G.(2009). Thermal behavior and stability of biodegradable spray-dried microparticles containing triamcinolone. *Int. J. Pharm.* 368, 45–55.
- El-Laithy, H.M.,Shoukry,O.,Mahran,L.G.(2011). Novel sugar esters proniosomes for transdermal delivery of vinpocetine: Preclinical and clinical studies. *Europ. J.Pharm. Biopharm*, 77(1),43-55.
- Feng,W.,Jian,Y.,Yu,S., Xing-Guo, Z., Fu-De, C., Yong-Zhong, D.,Hong,Y., Fu-Qiang, H.(2008). Studies on PEG-modified SLNs loading vinorelbinebitartrate (I):Preparation and evaluation in vitro. *Int.J.Pharm.* 359, 104-110.
- Freitas,C., Müller,R.H.(1999). Correlation between long-term stability of solid lipid nanoparticles (SLN<sup>(TM)</sup>) and crystallinity of the lipid phase. *Eur. J. Pharm. Biopharm.* 47, 125–132.
- Ghorab,M.M., Abdel-salam, H.M., Abdel-Moaty, M.M.(2004). Solid lipid Nanoparticles- effect of lipid matrix and surfactant on their physical characteristics. *Bull.Pharm.Sci.,Assiut University.* 27,155-159.

- Gupta,A.K.,Lynde ,C.W.,Kunynetz,R.A.W.,Amin, S., Choi,K.L.,Goldstein,E. ( 2003). A Randomized, Double- Blind, Multicenter, Parallel Group Study to Compare Relative Efficacies of the Topical Gels 3% Erythromycin/5% Benzoyl Peroxide and 0.025 % tretinoin/ Erythromycin 4% in the Treatment of Moderate Acne Vulgaris of the Face. *J.Cuten.Med. Surg*, 7 (1), 31- 37.
- Han,F., Li,S., Yin,R., Liu,H., Xu,L. (2008).Effect of surfactants on the formation and characterization of a new type of colloidal drug delivery system: Nanostructured lipid carriers. *Coll.Surf. A: Physico. Eng. Aspec* .315,210–216.
- Kim,B.D.,Na,K., Choi,H.K.(2005). Preparation and characterization of solid lipid Nanoparticles (SLN) made of cacao butter and curdlan. *Eur. J. Pharm.Sci.* 24, 199-205.
- Le Verger, M. L., Fluckiger,L., Kim,Y., Hoffman,M., Maincent,P.(1998).Preparation and characterization of nanoparticles containing antihypertensive agent. *Eur.J.Pharm.Biopharm*, 46, 137-143.
- Mehnert,W. , Mader,K. (2001). solid lipid Nanoparticles production, characterization and applications. *Adv. Drug. Deliv. Reviews*. 47, 165- 196.
- Motwani,S.K., Chopra,S., Talegaonkar,S., Konchan,K., Ahmed,F. J., Khar,R.K.(2008). Chitosan –sodium alginate nanoparticles as submicroscopic reservoirs for ocular delivery: formulation, optimization and in vitro chacterization .*Eur.J. Pharm.Biopharm*. 68,513- 525.
- Muhlen,A.,Mehnert,W. (1998).Drug release mechanism of prednisolone loaded solid lipid nanoparticles. *Pharmazie*. 53,552–555.
- Muhlen,A.,Schwarz,C.,Mehnert,W.(1998). Solid lipid nanoparticles (SLN) for controlled drug delivery–drug release and release mechanism. *Eur. J. Pharm. Biopharm*. 452,149–155.
- Muller,R.H.,Mader,K.,Gohla,S.(2000). Solid lipid nanoparticles (SLN) for controlled drug delivery - a review of the state of the art. *Eur. J. Pharm.Biopharm*, 50, 161- 177.
- Prabha,F.A., Zhou,W. Z., Panyam,J.,Labhasetwar,V. (2002).size dependency of nanoparticles-mediated gene transfer: studies with fractionated nanoparticles. *Int.J. Pharm*. 244, 105-15.

- Pretsch, E., Bühlmann, P., Badertscher, M. (2000). IR Spectroscopy. Structure Determination of Organic Compounds. Springer, Berlin Heidelberg, 267-320.
- Pretsch, E., Bühlmann, P., Badertscher, M. (2009). IR Spectroscopy. Structure Determination of Organic Compounds. Springer, Berlin Heidelberg, 1-67.
- Reddy, L. H., Murthy, R. S. (2005). Etoposide-loaded nanoparticles made from glyceride lipids: formulation, characterization, in vitro drug release, and stability evaluation. AAPS Pharm.Sci.Tech. 6, (2), Article 24.
- Sarisuta, N., Kumpugdee, M., Muller, B.W., Puttipipatkachorn, S. (1999). Physico-chemical characterization of interactions between erythromycin and various film polymers. Int.J.Pharm. 186, 109-118.
- Schafer- Korting, M., Mehnert, W., Korting, H.C. (2007). Lipid Nanoparticles for improved topical application of drugs for skin diseases. Adv. Drug. Deliv. Rev. 59, 427- 443.
- Schwarz, C., Mehnert, W., Lucks, J.S., Muller, R.H. (1994). Solid lipid nanoparticles (SLN) for controlled drug delivery. I. Production, characterization and sterilization . J. Cont.Rel, 30, 83-96.
- Stecova, J., Mehnert, W., Blaschke, T., Kleuser, B., Sivaramakrishnan, R., Zouboulis, C.C., Seltmann, H., Korting, H.C., Kramer, K.D., Shafer- Korting, M. (2007). Cyproterone Acetate Loading to Lipid Nanoparticles for Topical Acne Treatment: Particle Characterisation and Skin Uptake. Pharm.Res. 24(5), 991- 1000.
- Sznitowska, M., Gajewska, M., Janicki, S., Radwanska, A., Lukowski, G. (2001). Bioavailability of DZ from aqueous-organic solution, submicron emulsion and solid lipid nanoparticles after rectal administration in rabbits. Eur. J. Pharm. Biopharm. 52, 159-163.
- Vivek, K., Reddy, H., Murthy, R.S.R. (2007). Investigations of the Effect of the Lipid Matrix on Drug Entrapment, In Vitro Release, and Physical Stability of Olanzapine-Loaded Solid Lipid Nanoparticles. AAPS. Pharm.Sci.Tech. 8 (4); article 83.
- Yang, Y.Y., Wang, Y., Powell, R., Chan, P. (2006). Polymeric core-shell Nanoparticles for therapeutics. Clin.Exp.Pharmacol.Physiol. 33, 557-562.

### **Legends of figures**

**Fig. 1.**In-vitro release of DP from SLNs.

**Fig. 2.**In-vitro release of ER from SLNs.

**Fig.3.** In-vitro release of TA from SLNs.

**Fig.4.** SE micrograph for DP-SLNs formula F1.

**Fig.5.** SE micrograph for ER-SLNs formula F1.

**Fig.6.** SE micrograph for TA-SLNs formula F1.

**Fig.7.** TE micrograph for DP-SLNs formula F1.

**Fig.8.** TE micrograph for ER-SLNs formula F1.

**Fig.9.** TE micrograph for TA-SLNs formula F1.

**Fig.10.** FTIR spectrum of GMS (main component of SLNs).

**Fig (11):** FTIR spectra of DP, physical mixture and DP- SLNs (formula F1), displaced for better visualization.

**Fig (12):** FTIR spectra of ER, Physical mixture and ER- SLNs (formula F1), displaced for better visualization.

**Fig (13):** FTIR spectra of TA, Physical mixture and TA- SLNs (formula F1), displaced for better visualization.

**Fig (14):** DSC thermogram of GMS displaced for better visualization.

**Fig (15):** DSC thermogram of plain SLN (formula F1), displaced for better visualization.

**Fig (16):** DSC thermograms of DP, Physical mixture of DP and GMS and DP-SLNs(formula F1), displaced for better visualization.

**Fig (17):** DSC thermogramsof ER, Physical mixture of ER and GMS andER- SLN (formula F1), displaced for better visualization.

**Fig (18):** DSC thermograms of TA, Physical mixture of TA and GMS and TA-SLNs(formula F1), displaced for better visualization.

Figure 1

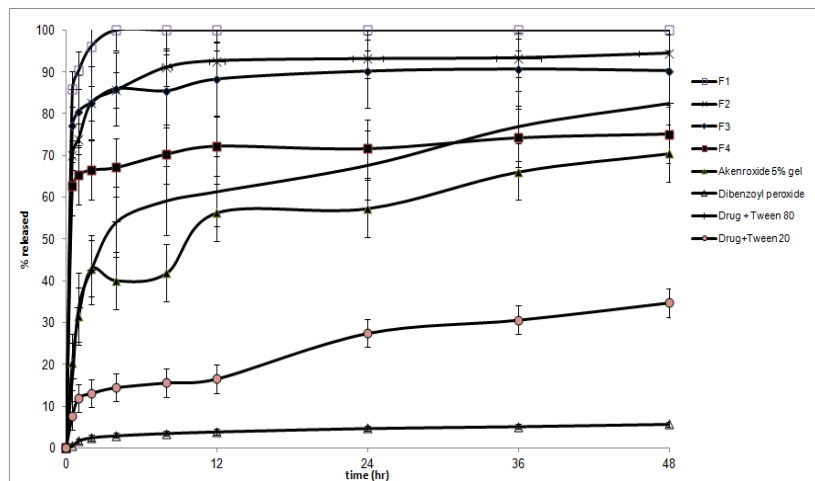


Figure 2

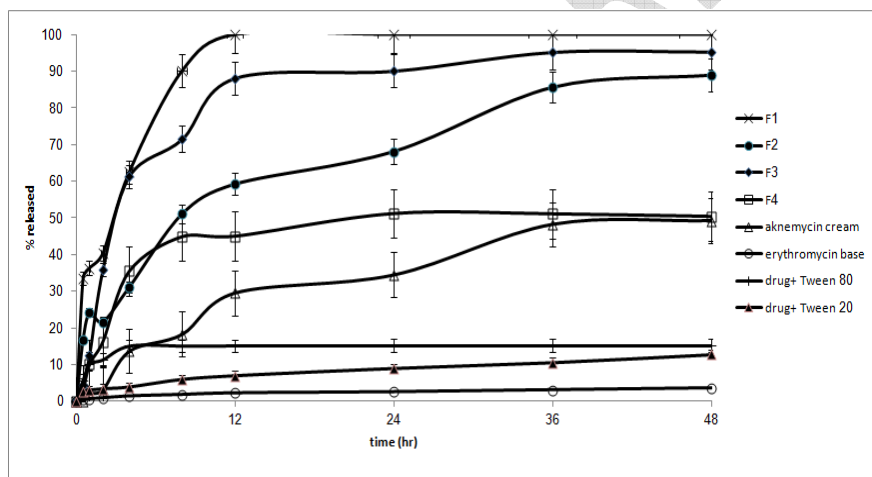


Figure 3

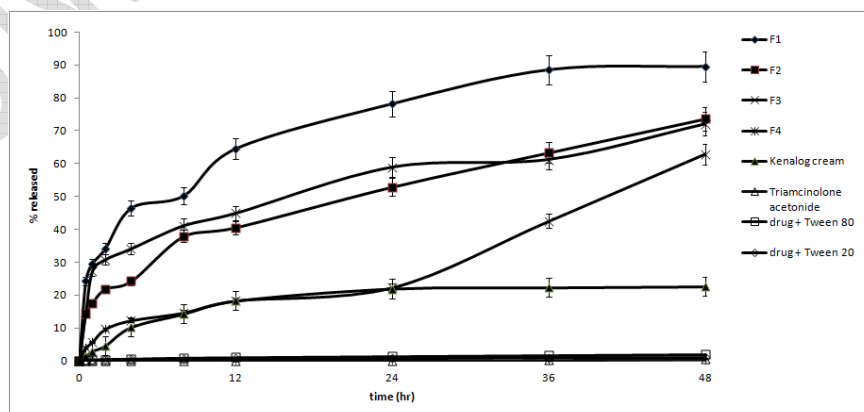


Figure 4

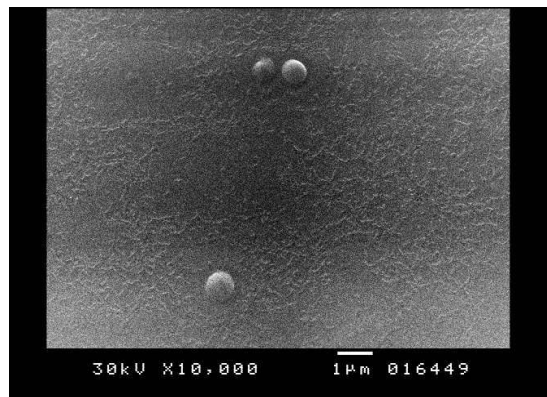


Figure 5

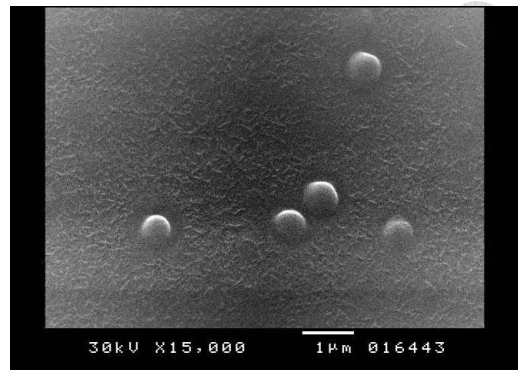


Figure 6

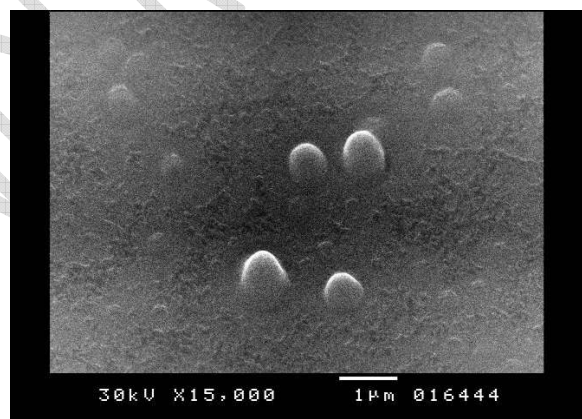


Figure 7

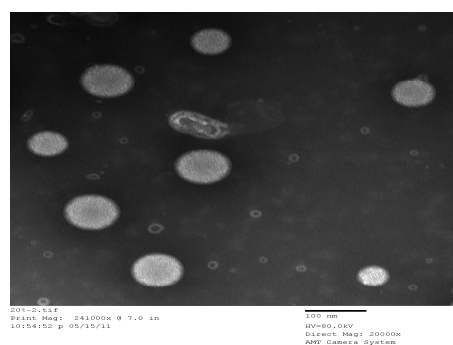




Figure 8

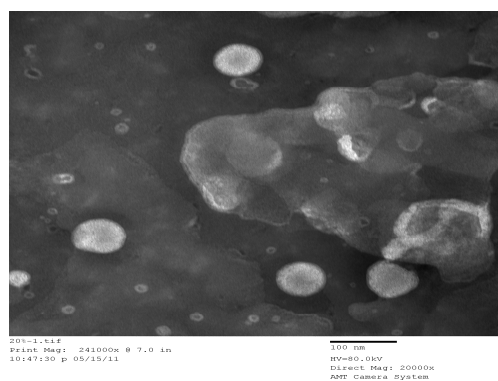


Figure 9

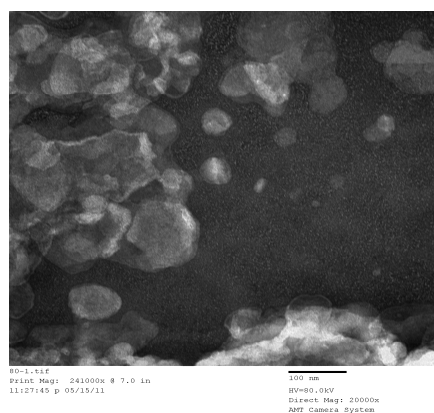


Figure 10

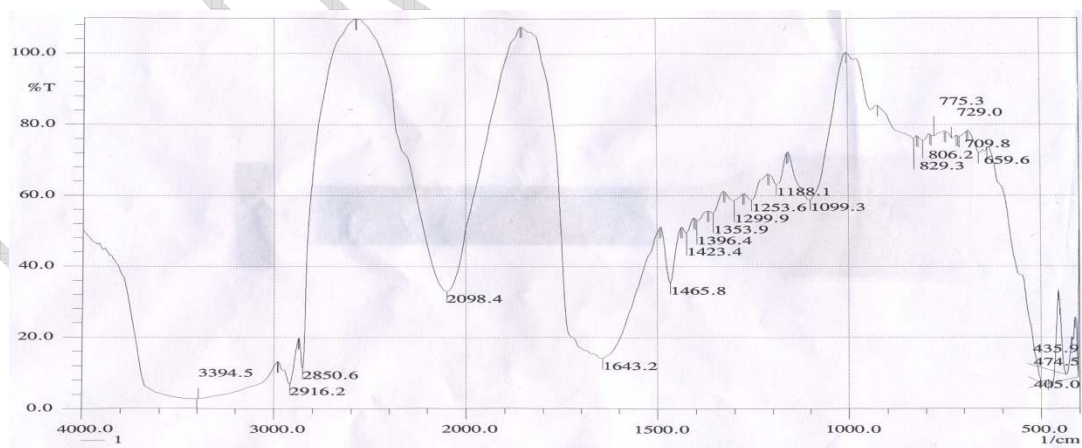




Figure 11

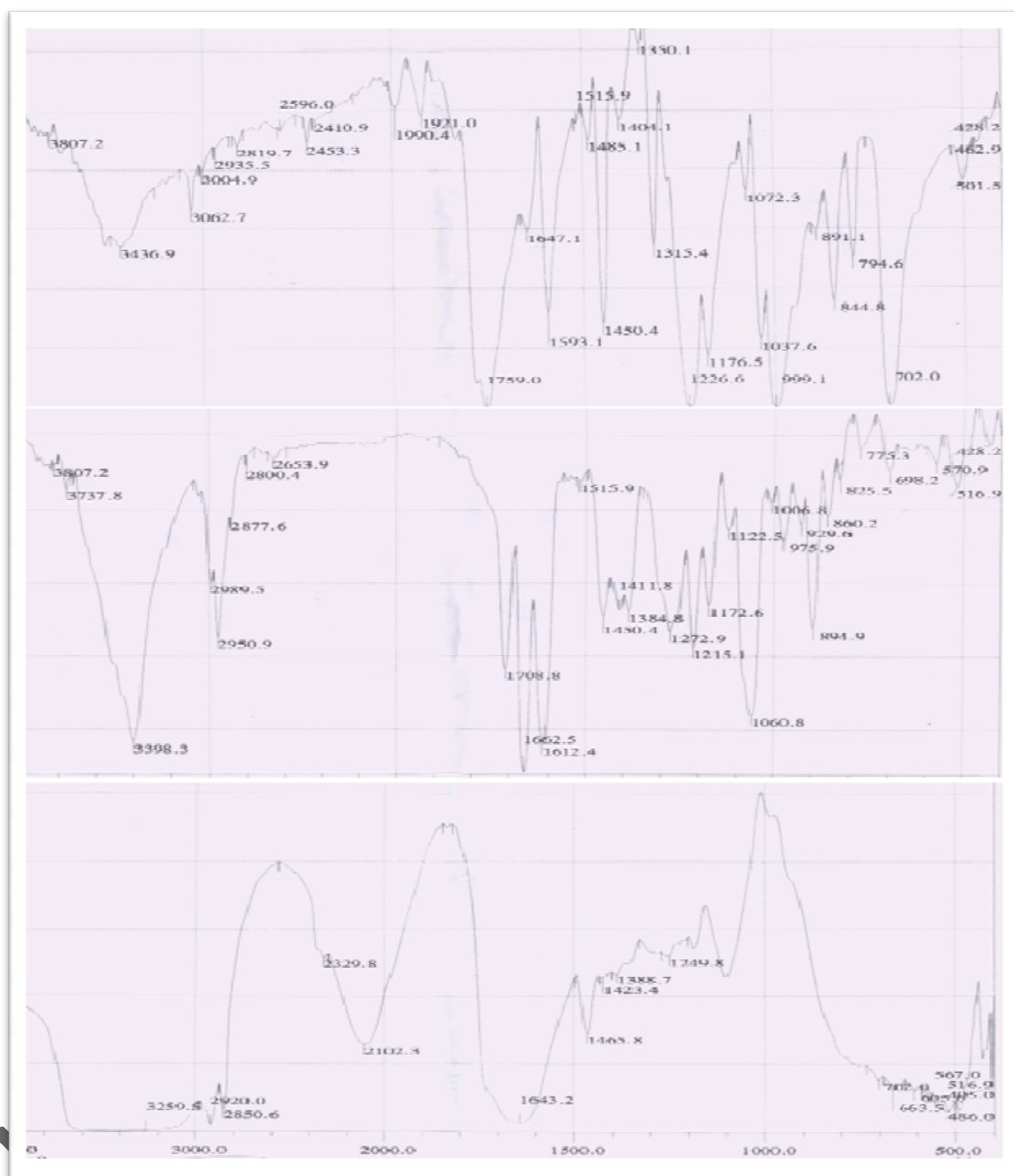


Figure 12

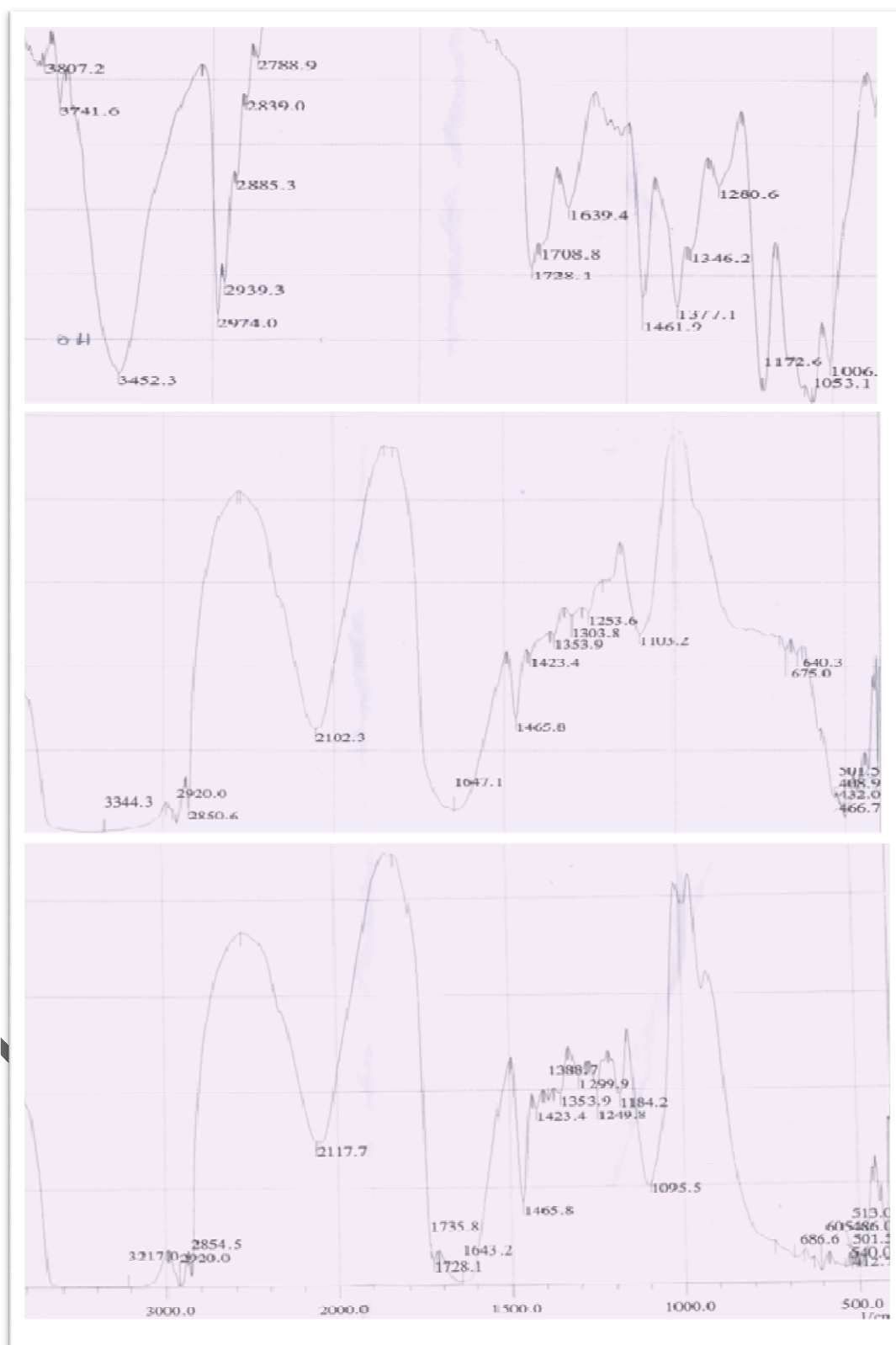


Figure 13

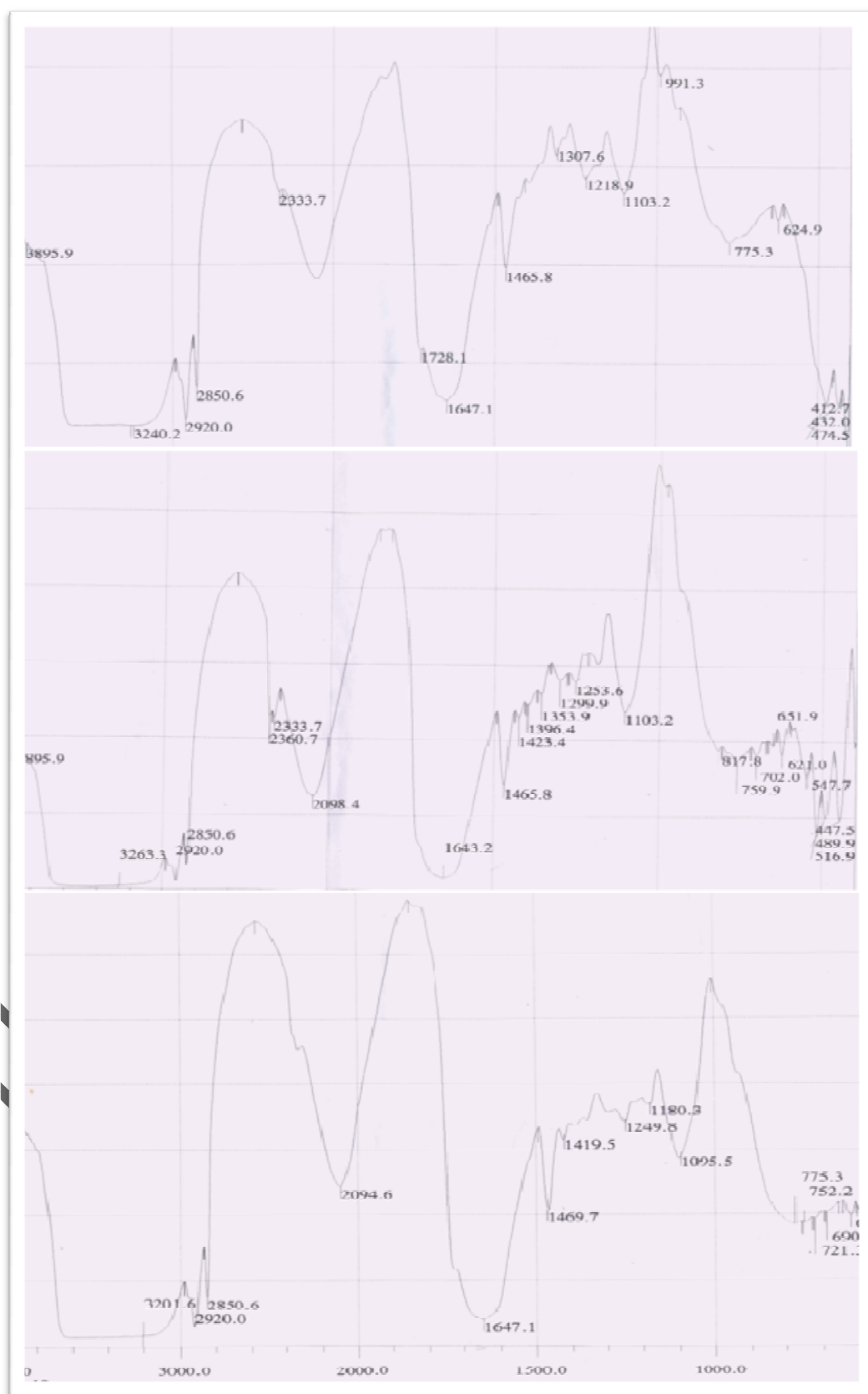


Figure 14

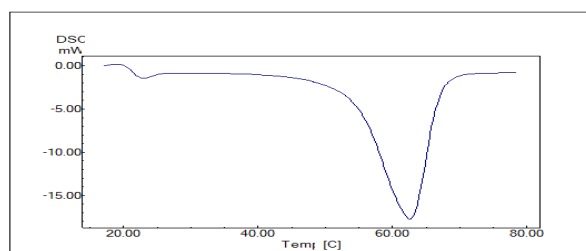


Figure 15

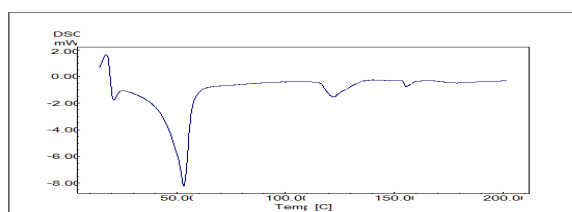


Figure 16

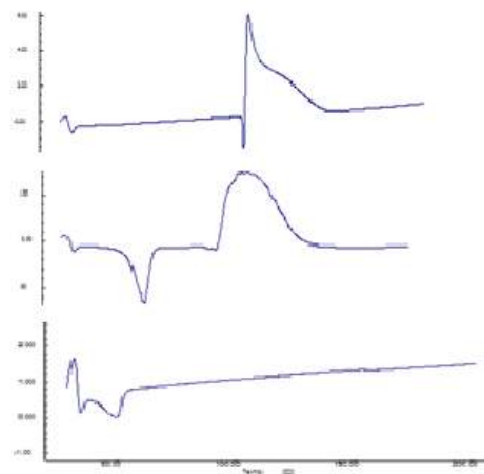


Figure 17

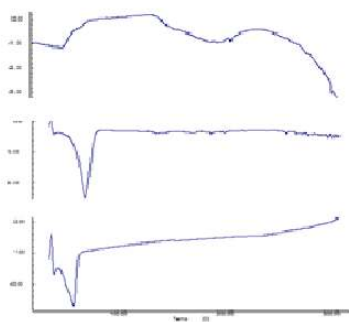


Figure 18

